

Nanoimprinted P3HT/C₆₀ solar cells optimized by oblique deposition of C₆₀

Yi Yang

Department of Physics, University of Texas at Dallas, Richardson, Texas 75083

Mukti Aryal

Department of Electrical Engineering, University of Texas at Dallas, Richardson, Texas 75083

Kamil Mielczarek

Department of Physics, University of Texas at Dallas, Richardson, Texas 75083

Walter Hu

Department of Electrical Engineering, University of Texas at Dallas, Richardson, Texas 75083

Anvar Zakhidov^{a)}

Department of Physics, University of Texas at Dallas, Richardson, Texas 75083

(Received 20 July 2010; accepted 11 October 2010; published 1 December 2010)

Poly(3-hexylthiophene) (P3HT)-C₆₀ organic photovoltaic devices with interpenetrating donor-acceptor interfaces were fabricated by oblique thermal deposition of C₆₀ into the P3HT nanogratings. The uniformity and step coverage of C₆₀ infiltration into the P3HT nanostructures, which can determine the device performance, were dependent on the C₆₀ evaporation angle. It was also observed that the C₆₀ deposition rate and thickness determine the efficiency. A 50% improvement in power conversion efficiency is observed due to the increased exciton dissociation rate at the larger area P3HT-C₆₀ interface at optimal C₆₀ deposition filling. With the proposed technique, a highly efficient organic solar cell using an insoluble acceptor has been fabricated. © 2010 American Vacuum Society. [DOI: 10.1116/1.3517513]

I. INTRODUCTION

In recent years, research in organic solar cells (OSCs) has been advanced tremendously, driven by the potential for low cost, large area devices with attractive market perspectives.^{1,2} One major challenge for OSCs is their relatively low power conversion efficiency (PCE), which is limited by the short exciton diffusion length in the photoactive layer.^{3,4} Although the bulk heterojunction (BHJ) architecture of OSCs is developed to increase the interfacial area between donor-acceptor components (and thus enhance exciton dissociation) and to greatly improve the efficiency, it is still inferior to other types of inorganic solar cells, which limits its commercialization. Finely controlled donor-acceptor phase separation, which is important for charge collection, is difficult to realize in a BHJ structure and can be responsible for the low PCE. A higher PCE for OSCs can be expected from nanoimprint lithography (NIL), which has emerged as a new technique to obtain both high charge separation and collection by ordered and continuously interdigitized active layer morphology,⁵⁻⁷ which is generally not possible using traditional techniques of spin coating and thermal annealing used in making BHJ devices. The ordered nanostructures by NIL also give permanent donor-acceptor phase separation and avoid the morphological degradation observed by others.⁸ For the nanoimprinted solar cells to obtain high performance, the complete infiltration of acceptor materials into the nanostructured donor polymer layer is critical in forming a good and large junction interface for efficient exciton dissociation, charge

separation, and collection. Previously, this was not possible due to either solubility problems or poor contact between patterned polymeric donor materials and vacuum deposited acceptor materials. Spin-coating is widely used for solvent-soluble acceptor, such as 1-(3-methoxycarbonyl)propyl-1-phenyl[6,6]C₆₁ (PCBM), but such process is limited by the availability of orthogonal solvent, material incompatibility, and spin-coating nonuniformity.

In this work, using oblique deposition, which is used to obtain conformal thin films with enhanced step coverage on

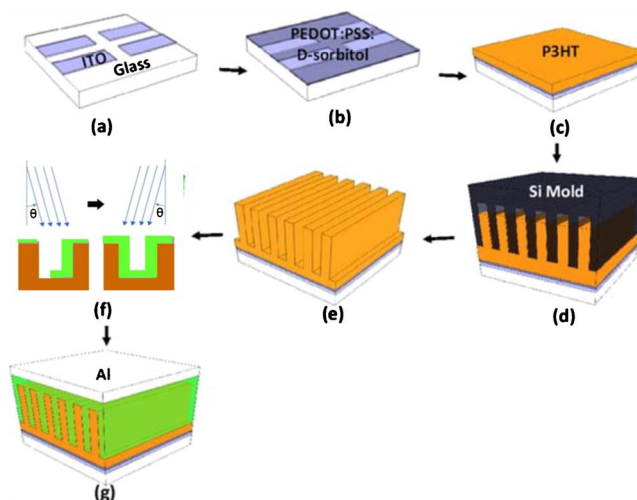


FIG. 1. (Color online) Schematic of (a) patterning ITO, (b) spin-coating PEDOT:PSS: D-sorbitol, (c) spin-coat P3HT, (d) nanoimprinting, (e) creating P3HT nanogratings, (f) thermal evaporating C₆₀, (g) depositing Al, and (h) oblique thermal evaporation of C₆₀ process.

^{a)}Electronic mail: zakhidov@utdallas.edu

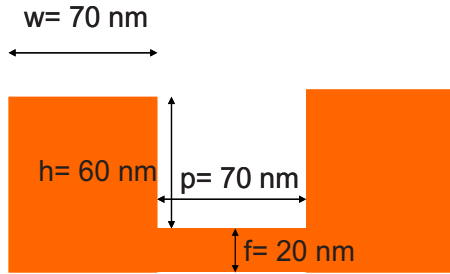


FIG. 2. (Color online) Schematic of P3HT grating with width $w=70$ nm, height $h=60$ nm, spacing $p=70$ nm, and residual layer $f=20$ nm.

patterned surfaces,⁹ we overcome the present problems for the fabrication of poly(3-hexylthiophene) (P3HT)/C₆₀ organic solar cell devices with good infiltration of C₆₀ into the nanoimprinted P3HT nanogratings, resulting in improved solar cell performance, further realizing the potential of NIL fabricated OSCs as a candidate for low cost renewable energy.

II. FABRICATION AND CHARACTERIZATION OF ORGANIC SOLAR CELLS

Solar cells were fabricated using imprinted P3HT nanogratings in the following structure of indium tin oxide (ITO)/poly(3,4-ethylenedioxythiophen):polystyrene sulfonic acid (PEDOT:PSS):D-sorbitol/P3HT/C₆₀/Al, as shown in Figs. 1(a)–1(g). ITO coated glass substrates were cleaned stepwise in acetone, toluene, and isopropyl alcohol under

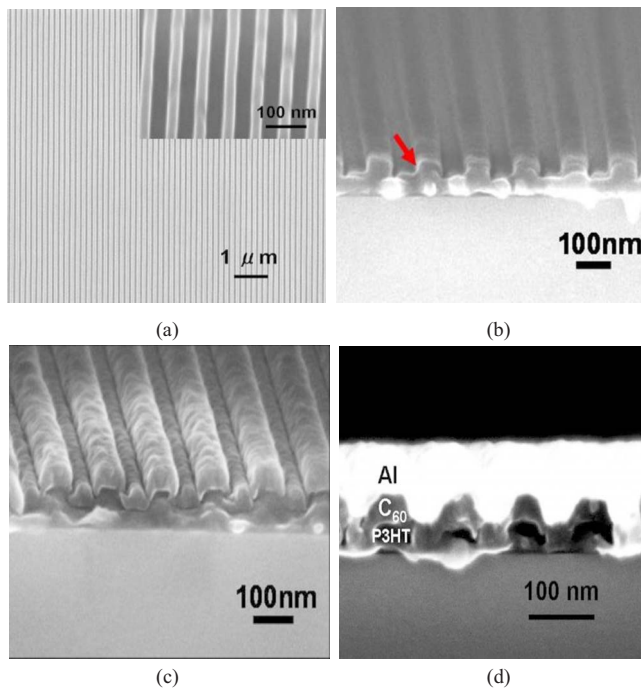


FIG. 3. (Color online) SEM images of (a) top view of P3HT nanogratings, (b) 20 nm C₆₀ deposition on P3HT nanogratings of $w=70$ nm, $p=70$ nm, and $h=60$ nm (with residual height of $R_h=20$ nm) from one direction where only one wall is covered (shown by arrow) (c) from both direction for complete coverage and (d) cross-section of P3HT nanogratings covered with C₆₀ and Al.

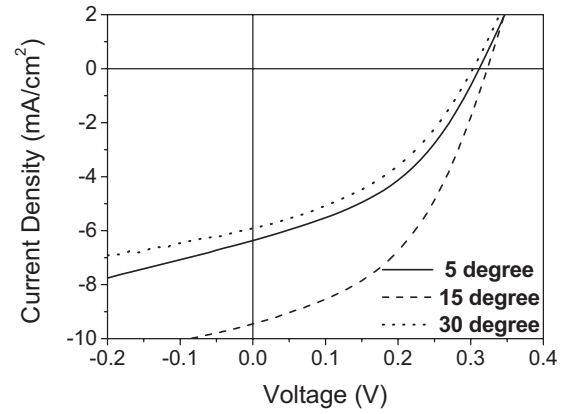


FIG. 4. I - V characteristics of nanoimprinted solar cells where C₆₀ was deposited on P3HT nanograting with oblique angles of 5° (solid), 15° (dash), and 30° (dot).

ultrasonication for 15 min each and subsequently dried by N₂. A thin layer (~ 20 nm) of PEDOT:PSS (H.C. Starck, Inc.) mixed with D-sorbitol (Aldrich) was spin-coated onto a cleaned ITO (Luminescence Technology) surface, which was prepared by ultraviolet ozone treatment for 5 min. After being baked at 150 °C for 15 min, 50 nm P3HT (Reike Metal, Ltd.) dissolved in chlorobenzene was spin-casted on top of the buffer layer. Nanograting structures of P3HT were formed by nanoimprinting using the nanolined Si mold according to a previously reported method.⁷ As shown in Figs. 2 and 3(a), at the height of P3HT gratings $h=60$ nm, the interface enhancement factor (IEF) is 1.86 [for grating width $w=70$ nm and spacing $p=70$ nm, $IEF=(w+p+2h)/(w+p)$], as compared with the planar P3HT layer. After the formation of nanograting P3HT structures, 40 nm C₆₀ was thermally evaporated into the P3HT nanostructures at the rate of 0.5 Å/s at different angles of 5°, 15°, and 30° to study the device performance dependence on the C₆₀ deposition angle. To get a complete and uniform coverage, C₆₀ was evaporated from two opposite directions separately, as shown in Fig. 1(f). The scanning electron microscopic (SEM) images of P3HT gratings coated with C₆₀ from one direction and both directions are shown in Figs. 3(b) and 3(c). The effect of C₆₀ deposition rate on power conversion efficiency was also studied by depositing 40 nm C₆₀ at 15° at varying rates of 0.5, 1, and 2 Å/s. The influence of C₆₀ thickness was studied by fixing the deposition angle at 15° and the rate at 0.5 Å/s but depositing C₆₀ with thicknesses of 20, 40, and 60 nm. Finally, 100 nm Al was thermally evaporated on the C₆₀ coated samples as the cathode, as shown in Fig. 3(d). Before

TABLE I. Summary of device performances for nanoimprinted solar cells at different C₆₀ deposition angles.

	V_{oc} (V)	J_{sc} (mA/cm ²)	FF	PCE (%)
5°	0.31	6.37	0.42	0.83
15°	0.32	9.46	0.45	1.35
30°	0.31	5.92	0.39	0.72

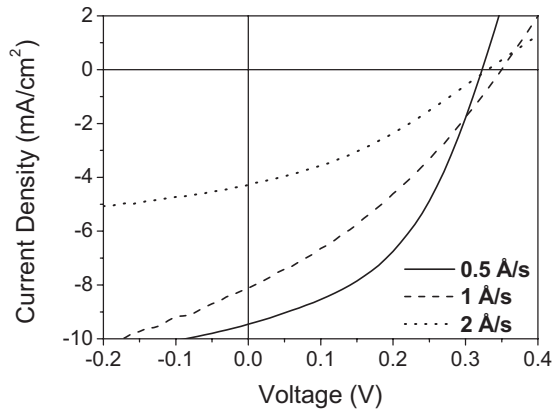


FIG. 5. I - V characteristics of nanoimprinted solar cells where C_{60} was deposited on P3HT nanograting with rates of 0.5 Å/s (solid), 1 Å/s (dash), and 2 Å/s (dot).

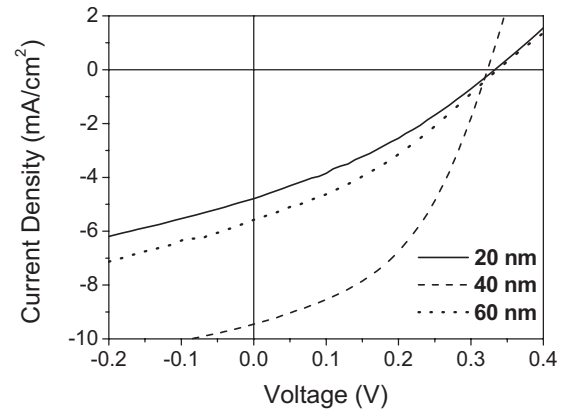


FIG. 6. I - V characteristics of nanoimprinted solar cells where C_{60} was deposited on P3HT nanograting with thicknesses of 20 nm (solid), 40 nm (dash), and 60 nm (dot).

measurement, all devices were annealed at 180 °C for 3 min in a N₂ filled glove box (<0.1 ppm O₂ and H₂O). After annealing, devices were tested in the same glove box using air mass 1.5 solar simulated light (AM 1.5G) at an intensity of 100 mW/cm².

The I - V curves of nanoimprinted devices at different C_{60} deposition angles are shown in Fig. 4. The open circuit voltage (V_{oc}), short circuit current density (J_{sc}), fill factor (FF), and PCE of these devices are listed in Table I. In our work, no visible C_{60} coverage differences on P3HT gratings are observed at these three deposition angles in SEM images, but the device performance is found highly dependent on them. The reason can be that without heating P3HT during C_{60} deposition, different deposition angles may lead to different interfacial contacts of C_{60} onto P3HT and also different degrees of C_{60} crystallization, which result in various device performances. Uniformity of C_{60} or defects may also be angle dependent. These effects of the deposition angle are being studied to better understand this phenomenon.

The I - V curves of nanoimprinted devices for C_{60} deposited at different rates are shown in Fig. 5. The V_{oc} , J_{sc} , FF, and PCE of these devices are listed in Table II. The device made at 0.5 Å/s rate shows a 120% increase in short circuit current and a 45% increase in fill factor, compared with that at 2 Å/s. This can be explained by possible defects in C_{60} induced at high deposition rate during evaporation, which has been observed by others.¹⁰

The I - V curves of nanoimprinted devices for different C_{60} thicknesses are shown in Fig. 6. The V_{oc} , J_{sc} , FF, and PCE of these devices are listed in Table III. The device for 40 nm

C_{60} shows the highest short circuit current and fill factor. This can be explained by the mobility imbalance between holes and electrons.¹¹ Typically for bilayer devices, the optimal donor and acceptor thicknesses are determined by the hole and electron mobilities, respectively. In this work, the residual P3HT thickness f is 20 nm and when C_{60} is 20 nm, the acceptor layer is too thin to balance the hole and electron currents. When C_{60} is 40 nm, the highest current and fill factor were obtained because of the matched currents. When it goes to 60 nm, the current and fill factor decrease due to high serial resistance of too thick C_{60} .

To prove the positive effect of nanoimprinting, similar process was used to fabricate planar bilayer unimprinted solar cells. The bilayer devices were composed of 40 nm C_{60} on 50 nm P3HT. The I - V curves of nanoimprinted and planar bilayer devices are shown in Fig. 7. The V_{oc} , J_{sc} , FF, and PCE of these devices are listed in Table IV. The solar cell built on imprinted P3HT gratings shows improved performance (50% increase in power conversion efficiency, 10% increase in fill factor, and 36% increase in short circuit current) over the unimprinted planar one. It is believed that the major reason is due to the finely controlled interpenetrated morphology with increased interface, which allows more efficient exciton dissociation and charge transport, as suggested by several theoretical studies.^{12,13} In our work, the increase in PCE is lower than that in IEF (50% increase in PCE compared with 86% increase in IEF), and the reason may be that the feature size of P3HT grating is larger than the exciton diffusion length and these are still current losses. Future work will be focused on how to further increase IEF by increasing the height and

TABLE II. Summary of device performances for nanoimprinted solar cells at different C_{60} deposition rates.

	V_{oc} (V)	J_{sc} (mA/cm ²)	FF	PCE (%)
0.5 Å/s	0.32	9.46	0.45	1.35
1 Å/s	0.34	8.12	0.33	0.93
2 Å/s	0.34	4.29	0.31	0.48

TABLE III. Summary of device performances for nanoimprinted solar cells at different C_{60} thicknesses.

	V_{oc} (V)	J_{sc} (mA/cm ²)	FF	PCE (%)
20 nm	0.34	4.79	0.31	0.51
40 nm	0.32	9.46	0.45	1.35
60 nm	0.34	5.58	0.33	0.63

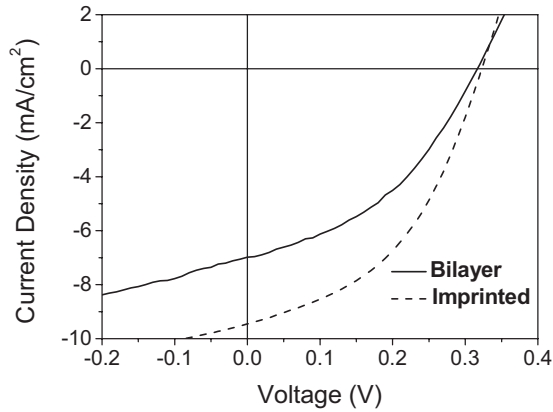


FIG. 7. I - V characteristics of bilayer unimprinted (solid) and nanoimprinted (dash) solar cells.

to improve the exciton dissociation by decreasing the width of P3HT gratings. The effect of P3HT residual layer thickness will also be studied to further increase the efficiency. At realistically achievable $h=2w$ and $w=p$, we expect more than 200% enhancement of PCE if good filling by C₆₀ or other acceptor component can be achieved.

III. CONCLUSION

Nanoimprinted P3HT/C₆₀ solar cells are fabricated by nanoimprinting P3HT nanogratings and their filling by oblique angle thermal deposition of C₆₀. Device efficiency is highly dependent on the C₆₀ deposition angle, rate, and thickness. Compared with flat bilayer device, nanoimprinted one shows 50% increase in power efficiency, which is due to larger interface in between, resulting in more efficient photogeneration by exciton dissociation on extended interfaces formed by finely controlled morphology. We expect 200% PCE enhancement if the height of P3HT gratings can be twice as their width.

TABLE IV. Summary of device performances for bilayer unimprinted and nanoimprinted solar cells.

	V_{oc} (V)	J_{sc} (mA/cm ²)	FF	PCE (%)
Bilayer	0.32	6.98	0.41	0.90
Imprinted	0.32	9.46	0.45	1.35

ACKNOWLEDGMENTS

The financial support of Welch Foundation Grant No. AT 16-17 and Rice/AFRL grant on “Hybrid solar cells” is highly appreciated. This work is also partially funded by NSF and AFOSR Grant No. FA-9550-05-1-04-09.

- ¹N. S. Lewis, *Science* **315**, 798 (2007).
- ²S. W. Tong, C. F. Zhang, C. Y. Jiang, G. Liu, Q. D. Ling, E. T. Kang, D. S. H. Chan, and C. X. Zhu, *Chem. Phys. Lett.* **453**, 73 (2008).
- ³J. E. Kroeze, T. J. Savenije, M. J. W. Vermeulen, and J. M. Warman, *J. Phys. Chem. B* **107**, 7696 (2003).
- ⁴P. Peumans, A. Yakimov, and S. R. Forrest, *J. Appl. Phys.* **93**, 3693 (2003).
- ⁵D. M. N. M. Dissanayake, A. A. D. T. Adikaari, and S. R. P. Silva, *Appl. Phys. Lett.* **92**, 093308 (2008).
- ⁶D. M. Nanditha, M. Dissanayake, Ross A. Hatton, Richard J. Curry, and S. R. P. Silva, *Appl. Phys. Lett.* **90**, 113505 (2007).
- ⁷M. Aryal, F. Buyukserin, K. Mielczarek, X. M. Zhao, J. M. Gao, A. Zakhidov, and W. Hu, *J. Vac. Sci. Technol. B* **26**, 2562 (2008).
- ⁸M. Jørgensen, K. Norrman, and F. C. Krebs, *Sol. Energy Mater. Sol. Cells* **92**, 686 (2008).
- ⁹T. Karabacak and T. Lu, *J. Appl. Phys.* **97**, 124504 (2005).
- ¹⁰D. Gupta, M. Bag, and K. S. Narayan, *Appl. Phys. Lett.* **92**, 093301 (2008).
- ¹¹A. L. Ayzner, C. J. Tassone, S. H. Tolbert, and B. J. Schwartz, *J. Phys. Chem. C* **113**, 20050 (2009).
- ¹²C. M. Martin, V. M. Burlakov, H. E. Assender, and D. A. R. Barkhouse, *J. Appl. Phys.* **102**, 104506 (2007).
- ¹³P. K. Watkins, A. B. Walker, and G. L. B. Verschoor, *Nano Lett.* **5**, 1814 (2005).